Ain Shams Engineering Journal 12 (2021) 1583–1594

Contents lists available at ScienceDirect

Ain Shams Engineering Journal

journal homepage: www.sciencedirect.com

Civil Engineering

Studying the impact of admixtures chemical structure on the rheological properties of silica-fume blended cement pastes using various rheological models

A. O. Habib [a], I. Aiad [b], F. I. El-Hosiny [c], Alaa Mohsen [a,*]

[a] Faculty of Engineering, Ain Shams University, Cairo, Egypt
[b] Egyptian Petroleum Research Institute (EPRI), Cairo, Egypt
[c] Faculty of Science, Ain Shams University, Cairo, Egypt

ARTICLE INFO

Article history:
Received 24 September 2020
Revised 26 December 2020
Accepted 27 December 2020
Available online 12 February 2021

Keywords:
Superplasticizers
Silica fume
Blended cement
Mini slump test
Rheometer test
Rheological models

ABSTRACT

In this study, the influence of various types superplasticizers namely; sikament-TG (TG), phenol-formaldehyde-sulfonilate (SI) and low phenol phenol-formaldehyde-sulfonilate (SII) on the rheological properties of silica fume-blended cement pastes (SF-BCPs) were studied. The mini slump and rheometer tests were used to examine the rheological properties of SF-cement blended pastes (SF-BCPs). The obtained results showed that, laboratory prepared admixtures (SI and SII) have a high efficiency than the commercial one (TG) in improving the rheological properties of SF-BCPs. Also, it is concluded that fresh control and admixed C-Ps exhibit a nonlinear behavior (shear-thin/thick). Therefore, Bingham-model cannot be applied for these C-Ps. Herschel–Bulkley-model and modified-Bingham- model can be used for shear-thick only as it is found that at $\tau=\infty$ when $\gamma^{\circ}=\infty$, while Hyperbolic-model can be applied for shear-thin only. The hyperbolic-model better than other models according to R^2 and RMSE values; thus, the obtained hyperbolic-model YS values tend to be more reliable.

1. Introduction

Over the last decades, utilizing chemical and mineral admixtures are widely used to change the physico-chemical properties of fresh and hardened C-Ps, to be used in several applications such as manufacturing of self-compacting concrete (SCCs) and Ultra-High Performance Concrete (UHPCs) [1,2].

SCCs are concretes that compacting under their weight only, therefore they can fill the whole pores with a great compact, resulting in decreasing the permeability and then increasing the durability [3]. Using high range water reducer (HRWR) admixtures is very important to produce SSCs [4]. Usually the SSCs have a high strength due to their dense structure. To increase the performance of SSCs, combination between chemical and mineral admixtures as blast furnace slag (BFS), fly ash (FA) and silica fume (SF) is used [5].

Owing to the differences in chemical composition and physical properties of mineral admixtures, they have diverse effects on the durability, mechanical, physico-chemical and rheological properties on concrete matrix [6].

SF is very fine particles can fill the pores and also, it can react with calcium hydroxide (CH) to produce additional amounts of calcium silicate hydrate (CSH). So, SF is used in the production of UHPCs [7,8]. The drawback in utilizing SF is its high surface area that consumes a high amount of water leading to workability reduction [9]. Therefore, using chemical admixtures in SF blended cement pastes is a very essential process.

The chemical admixtures are used to improve the rheological behavior of cement slurries by dispersing the agglomerated cement particles and hydrating products. There are many mechanisms for the dispersion effect of chemical admixtures, one or more can occur simultaneously such as: (i) formation of lubricating layers between cement grains; (ii) leaving more free water used to improve the workability by inhibiting hydration of cement surface; (iii) making electrostatic repulsion force by creating negative charge on the cement particles; (iv) induced steric hindrance by

* Corresponding author.
E-mail address: alaa.mohsen@eng.asu.edu.eg (A. Mohsen).
Peer review under responsibility of Ain Shams University.

Production and hosting by Elsevier

https://doi.org/10.1016/j.asej.2020.12.009
2090-4479/

forming long graft side chains, prevent particles contact; and (v) reduced the surface tension of water. The dispersion mechanism of admixture is depending on type of cement, type and dose of admixture, mixing methods and temperature.

Investigation the rheological properties of the C-Ps is very essential for mixing procedure, placement, and the economical proportioning. Determination of flow properties is affected on: (i) consolidation; (ii) ease of placement; (iii) strength and durability; (iv) setting time and; (v) consistency. Therefore, controlling the rheological properties of the cement slurries is very essential for methods of mixing and placement as well as the economical proportioning [10]. (Heikal M., et al., 2005) study the effect of partial substitution of by 10% SF on the rheological properties of SF-BCPs, it was found that addition of SF leads to an increase in shear stress values. Superplasticizer is required to decrease of the shear stress of the cement pastes. As the temperature increases, the shear stresses decrease with the increase of shear rate [11].

Rheologists described the concrete as very complicated materials to study its rheological properties [12], as its behaviors are not only shear dependent, but also time dependent due to hydration with YS and plastic viscosity [6,12–14]. Therefore, it is so difficult to predict the possibility of flow behavior by using one rheological model [6,15]. Different mathematical models (e.g., power-low-model, Bingham-model, power law with YS model [Herschel–Bulckley- model], binomial equation of second order [Atzeni-flow-model or Modified-Bingham- model], Casson-model, Hyperbolic-model, etc.) are used to describe the rheological behavior of C-Ps whether shear thinning or thickening (sh-thin/thick) behaviors [16]. Each model is suitable for an exact material and at definite range of measurements [6]. Also, the calculated rheological parameters can vary significantly by using different models [6,17].

One of the important parameters that affected on the selection of a suitable model is the chemical composition of starting materials. Mohamed A. S., 2017 concluded that a nonlinear model was effective in case of studying the rheological properties of oil well cement modified with nano clay [18]. Also, when the effect of temperature on the rheological properties of a water-based bentonite drilling mud modified with iron oxide nanoparticle was investigated. It was predicted that, the hyperbolic model predicted the shear thinning relationship between the shear stress and shear strain rate of the nano Fe_2O_3 modified bentonite drilling mud very well. Also, the hyperbolic model has a maximum shear stress limit whereas the Herschel–Bulkley model did not have a limit on the maximum shear stress [19].

The current framework aimed to explore the effect of two laboratory prepared additives (SI and SII) and commercial one (TG) on the rheological properties of SF-BCPs at different temperatures 25, 45 and 65 °C. Also, some mathematical models were studied such as Bingham-model, Herschel–Bulckley model, Modified-Bingham-model, and Hyperbolic-model to choose the suitable model to be applied in this work.

2. Materials and experimental program

2.1. Materials

2.1.1. Blended cement

Blended cement pastes prepared from dry mixing of ordinary Portland cement (OPC) with 7.5% SF by weight was used in this work. The cement was mixed with SF mechanically using a porcelain ball mill for two hours to assure complete homogeneity of the mixture. The OPC and SF were delivered from Suez Cement Company and Sika Egypt Company, Egypt; respectively. The blaine-surface area of OPC is 3450 cm^2/g and of SF is 20200 cm^2/g. The chemical composition of OPC and SF is scheduled in Table 1. The phase composition of the cement was calculated using Bouge's equation and was 52.0% C_3S, 19.2% β-C_2S, 8.8% C_3A and 11.1% C_4AF.

2.1.2. Chemical admixtures

The polymeric additives used in this study are SI & SII which were laboratory prepared. SI admixture was synthase by adding 133 g of phenol (C_6H_5OH), 96 g of sulfanilic acid sodium salt ($C_6H_6NO_3SNa$) and 400 ml water to a reaction vessel equipped with a stirrer. The alkalinity of this mixture was adjusted at pH = 9 by using 20% aqueous sodium hydroxide (NaOH). The solution mixture was heated and stirred to 90 °C, then 168 g of 37% aqueous formaldehyde solution (HCHO) was added drop by drop into the reactor vessel. The reaction was finished after 3.5 h. Then the prepared solution was cooled to ambient temperature and adjusted to pH 11.0 with 20 wt% aqueous NaOH. The same method was used to prepare SII but with reducing the amount of phenol to half the weight of SI (66.5 g of phenol) [9].

Figs. 1–2 shows the chemical structure and FT-IR of the synthesized polymers, respectively. The FTIR test was conducted by using JASCO FT/IR- 6100 Spectrometer in the region from 500 to 4000 cm^{-1}. The matching between the prepared admixtures and reference spectra was according to Sigma- Aldrich library [20]. Also, a commercial TG admixture supplied from Sika Egypt Company was used, to evaluate the efficiency of the prepared additives in enhancing the rheological properties of C-Ps. The exact chemical structure of TG is unknown due to the confidential commercial information, but from its data sheet it is prepared as modified naphthalene-based admixture (Fig. 3). The physical properties of these admixtures are represented in Table 2. Mw (weight average molecular weight) and Mn (number average molecular weight) were determined by using gel permeation chromatography (GPC).

2.2. Experimental program

2.2.1. Rheological measurements

The rheological properties of SF-BCPs were studied using two different procedures, namely, Mini-slump test and Rheometer test.

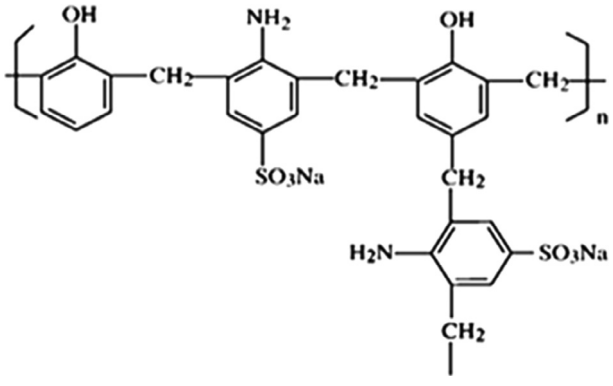

Fig. 1. Chemical structure of the synthesized admixtures (SI and SII).

Table 1
The chemical composition of the used OPC and SF.

	SiO_2	Al_2O_3	Fe_2O_3	CaO	MgO	SO_3	K_2O	Na_2O	LOI	Total
OPC	20.35	3.75	3.63	60.82	1.64	3.68	0.16	0.42	4.31	98.76
SF	94.81	0.16	0.84	0.89	0.49	0.08	0.2	0.05	2.43	99.95

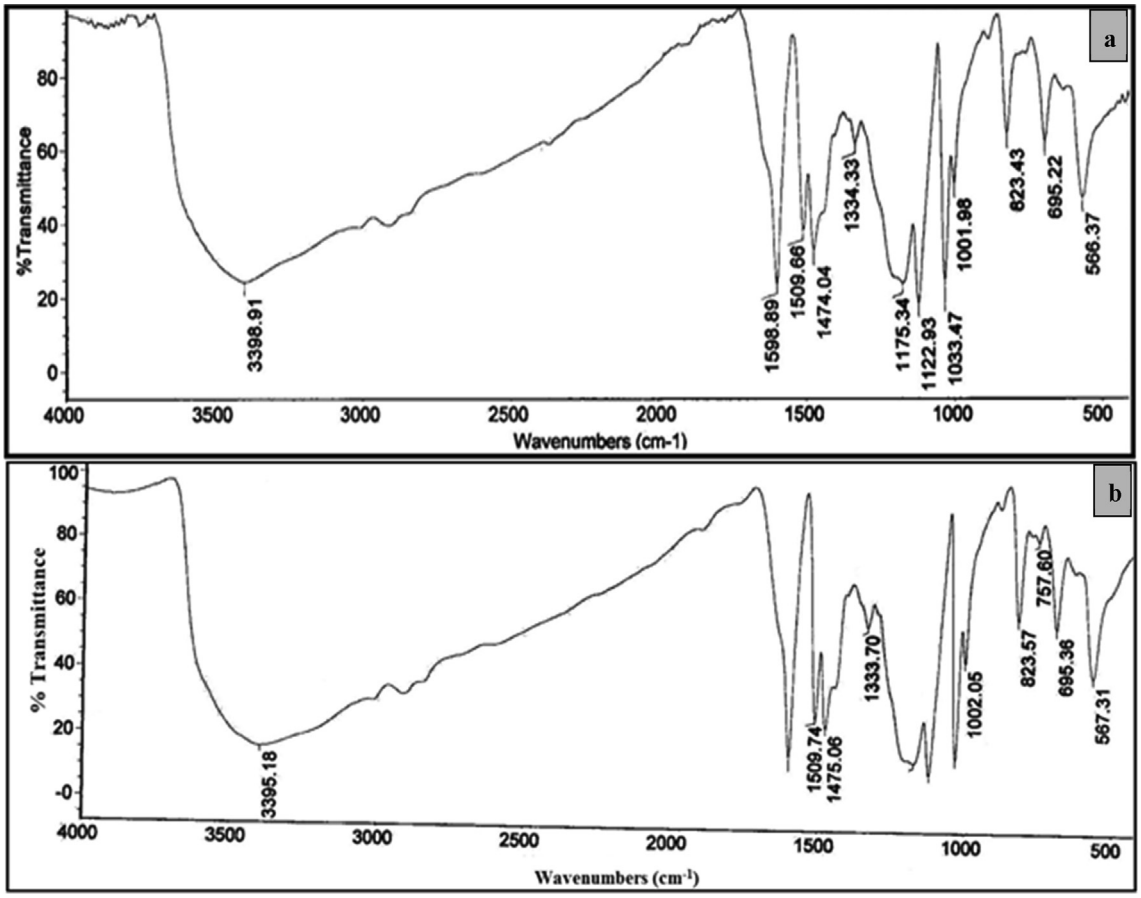

Fig. 2. FT-IR spectroscopic analyses of the synthetic admixtures (a) SI and (b) SII.

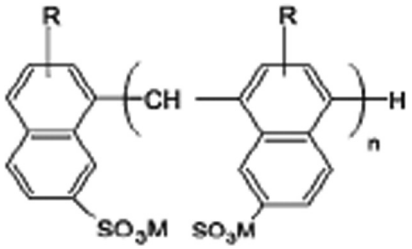

Fig. 3. Chemical structure of the modified naphthalene-based admixtures (TG).

Table 2
The physical properties of chemical admixtures (TG, SI and SII).

	Density	Mw	Mn
TG	1.18	8853	7129
SI	1.2	9979	7817
SII	1.25	11,136	10,021

2.2.1.1. Mini-slump test. The mini-slump procedure was used for characterizing the pastes and grouts rheological activity. In this test, constant water/solid (W/S) ratio of 0.38 with different admixtures doses (0.00, 0.25, 0.50, 0.75 and 1.00 cement mass percent) was used in this study. The paste was stirred using a mechanical stirrer for three minutes and then poured into a metallic cone (Abram's cone) that used for regular slump tests but with small dimension (top diameter of 20 mm, bottom diameter of 40 mm and height of 60 mm). The cone was put on metallic plate above vibrated table then it is vertically removed. The paste flowed under its own mass forming a pancake shape. The average spread diameter of the pancake form was measured [21,22].

2.2.1.2. Rheometer test. The SF-BCPs were prepared by using blender-mixer in which cement was mixed with water containing admixtures according to the following method. The W/S ratio was fixed at 0.4 and the admixtures doses used were (0.00, 0.25, 0.50 and 0.75 cement mass percent). Firstly, the required water and chemical admixture were mixed for 15 sec at a slow speed to ensure presence of complete homogeneity between them. The blended cement was added to admixture solution over a period of 15 sec. For another 15 sec, the blended cement was manually mixed by using a rubber spatula to homogenize the material sticking to the mixing container wall with the rest of the paste. Finally, the mixing resumed at high speed (100–120 rpm) for another 45 s followed by 1 min rest and another 1 min by the previous speed. The rheological measurements were then performed with rotating coaxial viscometer (Rheocalc V3.3 Build 49-1, Spindle used is SC4-25, Brookfield viscometer, USA). The slurry was transferred into the measuring cell. The method was based on measuring the shear stress (SS) against the shear rate (SR), the SR values were 2.20, 6.60, 11.00, 15.40, 19.80, 24.20, 28.60, 33.00, 37.40, 41.80, 46.20, 50.60 and 55.00 S^{-1}. This test was repeated for all C-Ps at different temperatures 45 °C and 65 °C, to show the effect of elevated temperatures on the rheological properties of the control and admixed SF-BCPs.

2.2.2. Rheological modeling

Several mathematical models' equations like Bingham-model, Herschel–Bulckley, Modified-Bingham and Hyperbolic-model were

used to calculate different rheological parameters as demonstrated in equations (1)–(4).

$$\tau = \tau^{\circ} + \mu\gamma^{\circ} \quad (\text{Bingham} - \text{model}) \tag{1}$$

$$\tau = \tau^{\circ} + k\gamma^{\circ n} \quad (\text{Herschel} - \text{Bulckley} - \text{model}) \tag{2}$$

$$\tau = \tau^{\circ} + \mu\gamma^{\circ} + a\gamma^{\circ 2} \quad (\text{Modified} - \text{Bingham} - \text{model}) \tag{3}$$

$$\tau = \tau^{\circ} + \frac{\gamma^{\circ}}{(A * \gamma^{\circ}) + B} \quad (\text{Hyperbolic} - \text{model}) \tag{4}$$

where τ: shear stress, τ°: yield stress, μ: viscosity, γ°: shear rate, k: fluid consistency index (correction parameter), n: flow behavior index, a: empirical physical parameter (second order parameter) and A&B: physical model parameters.

The choice of an effective model to be implemented depends on the conditions set out in Table 3 being satisfied. Also, comparison occurs between these models by using R^2 and RMSE to determine the accuracy of the model and show which one gives the best fitting.

$$R^2 = \left(\frac{\sum_i (x - x^{\circ})(y - y^{\circ})}{\sqrt{\sum_i (x - x^{\circ})^2} * \sqrt{\sum_i (y - y^{\circ})^2}} \right)^2$$

$$\text{RMSE} = \sqrt{\frac{\sum_{i=1}^{n} (y^{\circ} - x^{\circ})^2}{N}}$$

where x: calculated value from the model, x°: mean of calculated values, y: actual value, y°: mean of actual values and N: number of data point.

3. Results and discussions

3.1. Mini-slump test

The mini-slump test is the most important test that can be used to estimate the workability of C-Ps. It was observed that the flowability of all admixed C-Ps is higher than the control sample as graphically represented in Fig. 4. Also, the workability increased with increasing the admixtures dose, which showed the effect of these admixtures in improving the workability of C-Ps without adding further excess water [21].

TG, SI and SII improve the flowability of C-Ps due to their steric hindrance and electrostatic repulsion effects. The steric hindrance effect is dependent on polymer side chain length. The electro static repulsion forces is due to creation of a negative charge [21] that results from production of SO_3^{2-} group on the cement grains, resulting in breakdown of agglomerates cement particles and decreases the viscosity of the pastes.

The spread area values of TG containing pastes are lower than both of SI and SII at the same doses, as the steric hindrance action is more effective in case of SII than SI than TG which is compatible with Mw and Mn results. Fig. 4 showed a linear increasing in the initial flowability at low doses of admixtures, followed by a plateau where the further admixtures fail to change flowability. The dose at which the pastes arrive to maximum flowability is called critical dose, in case SII is lower than SI lower than TG.

Table 3
Conditions that must be satisfied by the model to represent the shear thinning/thickening behavior.

For shear thinning (n < 1)	For shear thickening (n > 1)
$\tau = \tau^{\circ}$ when $\gamma^{\circ}=0$	$\tau = \tau^{\circ}$ when $\gamma^{\circ}=0$
$\frac{d\tau}{d\dot{\gamma}} > 0$	$\frac{d\tau}{d\dot{\gamma}} > 0$
$\frac{d^2\tau}{d\dot{\gamma}^2} < 0$	$\frac{d^2\tau}{d\dot{\gamma}^2} > 0$
At $\gamma=\infty \Longrightarrow \tau$ = value	At $\gamma=\infty \Longrightarrow \tau=\infty$

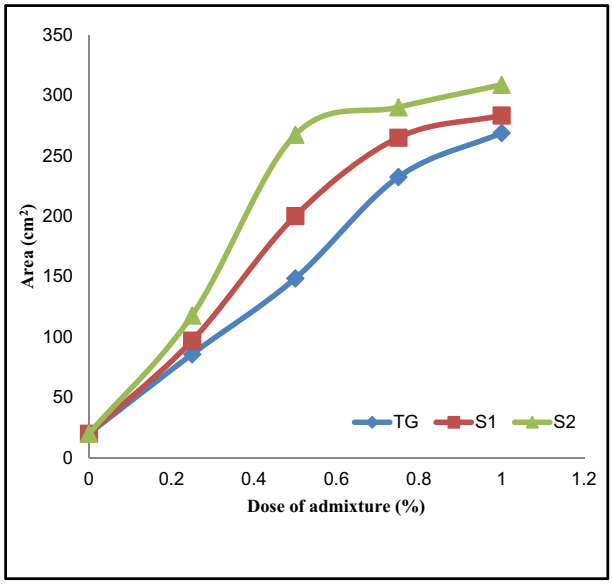

Fig. 4. The mini-slump values of SF blended cement slurries admixed with different doses of different admixtures as well as control slurry.

3.2. Rheometer test

3.2.1. Effect of applied shear rate on the shear stress values of admixed SF blended cement pastes

3.2.1.1. Rheological characteristics of control and admixed cement pastes at room temperature. Rheological tests are used in designing processing equipment such as selecting the appropriate pump to give enough power for flowing a material over a certain distance in pipelines. The relation between SR and SS for control and admixed C-Ps from low to high SR was measured at 25 °C and the data are illustrated in Fig. 5. It was indicated that for all C-Ps, the SS values increased with increasing the SR [10]. As the dose of admixtures increased the SS values decreased (the flow curve shift to lower yield values as compared to that control sample), indicating that such admixed pastes required a lower energy to flow compared to control sample, as these admixtures prevent formation of flocculated structures which reflects their powerful dispersion action [16,23–25]. This is attributed to the electrostatic repulsion and/or steric hindrance effect as discussed before, resulting in increasing the inter-particles spaces between the flocculated structures leading to a high fluidity [16,26–30].

Adsorption of the used chemical admixtures on the surface of cement grains and, on the nuclei of hydration products inhibits water to contact with excess cement grains, that resulting in presence of more free water between cement particles which causes enhancing in the flowability.

Fig. 5 showed lower SS and YS values for SII admixed C-Ps than SI than TG. SII has a high fluidity than SI reflecting the chemical structure effect of admixtures. The effect of the side chains on the fluidity of the C-Ps is still debatable issue. It was informed that, increasing the graft chains length, a higher fluidity of the C-Ps is obtained [31]. Conversely, it was specified that co-polymer with long graft chains attain high fluidity which is rapidly lost while that with short graft chains retain the fluidity for a long time [32]. The chemical structure of SI and SII is composed of linear

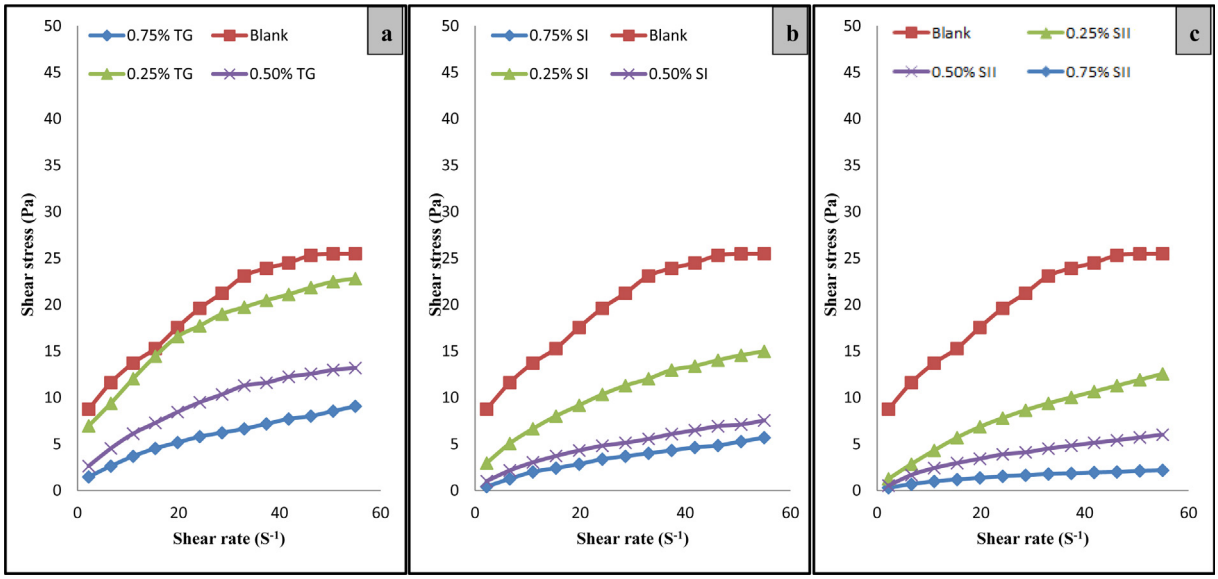

Fig. 5. Shear stress-shear rate relationship for cement pastes containing various doses from TG, SI and SII at 25 °C.

hydrophobic trunk polymer containing (SO_3^{2-}) group that enhance adsorption of admixture molecules to the surface of cement particles, and side chains of phenol–formaldehyde are directed to the bulk of the pore solution. SI has a long polymer chain which may hinder the dispersion on the cement grains leading to high rheological parameters.

3.2.1.2. Rheological characteristics of control and admixed cement pastes at elevated temperatures. Studying the temperature effect on the fluidity behavior for the control and admixed C-Ps is very important to know the limitation during placement and transportation. As temperature is altered, the rheological properties of cement pastes are also altered [27].

The rheological parameters of the SF-BCPs under the effect of different temperatures (45 °C and 65 °C) were studied. The SS values at different SR values at these temperatures were plotted in Figs. 6–7.

As shown in Figs. 6a, 7a, the C-Ps admixed with different doses of TG have lower SS values than the control pastes at all temperature. As the doses of TG increased, the SS values decreased at low SR (<37.4 S^{-1} at 45 °C and < 33 S^{-1} at 65 °C). At a higher SR (>37.4 S^{-1} at 45 °C and > 33 S^{-1} at 65 °C), it was found that a 0.75% TG has a higher SS value than 0.50% TG. This is due to desorption of adsorbed polymer at a high SR, thus the concentration of polymer increases in the interstitial solution, leads to increase the viscosity of solution [33]. So, as the doses of admixture increase in the interstitial solution the viscosity increase. This indicated that at a high temperature only, the layer of admixture that formed on the cement particles can break down leading to increasing the rate of hydration [34].

Also, SI and SII admixed C-Ps have lower SS values than the control pastes at all temperature (45 °C and 65 °C) as reported in Figs. 6b, c, 7b, c; respectively. In case of SI, as the doses increase the SS values decrease at a low SR (<41.8 S^{-1}). But at a SR higher

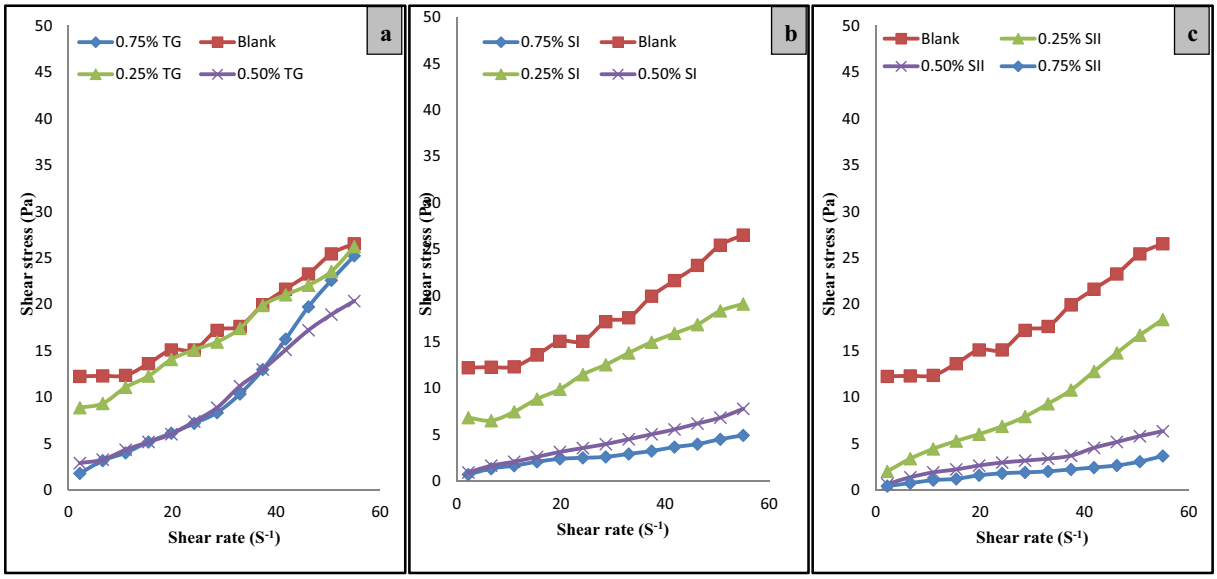

Fig. 6. Shear stress-shear rate relationship for cement pastes containing various doses from TG, SI and SII at 45 °C.

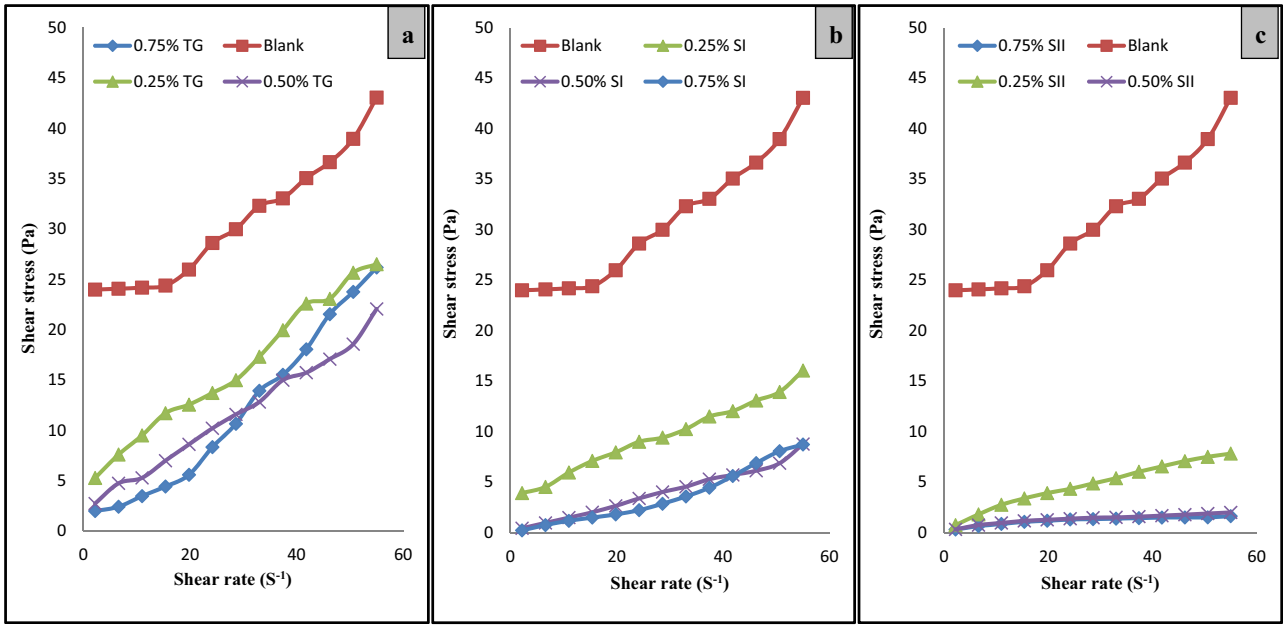

Fig. 7. Shear stress-shear rate relationship for cement pastes containing various doses from TG, SI and SII at 65 °C.

than 41.8 S^{-1}, the SS of 0.75% SI is higher than 0.50% SI. In case of SII, the SS values decrease with increasing the doses of SII at all SR values. This indicates that SI and SII have a high stability against temperature with increasing the SR.

3.2.2. Application of different rheological models

Different mathematical models illustrated above were used to describe the rheological behavior of C-Ps. It was noted that the calculated rheological parameters can vary significantly by using different models [6,17].

3.2.2.1. Bingham-model. Bingham-model is the simplest model. It is used to evaluate the rheological properties of cement paste [12,13,35]. As shown in Table 4, applying this model to the data obtained from different mixes resulted in a negative YS values which are physically impossible; this is due to a high error obtained in the fitting curve [35]. Also, it can't be valid to deduce the rheological properties of these C-Ps [35,36] because of their non-linear behavior as obtained in the Figs. 5–7 (sh-thin/thick depends on the dose of admixtures and condition of measurement) [18,19,35–37]. Therefore, an additional parameter must be added to solve the problems of Bingham-model. Two models have been used to characterize this relationship which are Herschel–Bulkley-model modified-Bingham-model [12,15,35,38,39].

3.2.2.2. Herschel–Bulckley-model. Herschel–Bulckley-model delivers a better fit of the test data, comparing with Bingham-model. For a nonlinear flow relationship viscosity isn't constant, so, the assumption of constant plastic viscosity is not used [18,19] and it replaced by apparent viscosity. Therefore sh-thin/thick behavior can be predicted from Herschel–Bulkley-model [36,40].

As illustrated above the model must satisfy the conditions that listed in Table 3, to be sure that the selected model is suitable for these pastes.

$$\frac{d\tau}{d\gamma} = k * n * \gamma^{(n-1)}$$

$$\frac{d^2\tau}{d\gamma^2} = k * n(n-1) * \gamma^{(n-2)}$$

Table 4
Rheological parameters of Bingham model for control and admixed cement pastes containing different doses from TG, SI and SII at different temperatures 25 °C, 45 °C and 65 °C.

Temperature(°C)	Dose (%)	Bingham model											
		TG				SI				SII			
		τ°	μ	R^2	RMSE	τ°	μ	R^2	RMSE	τ°	μ	R^2	RMSE
25 °C	0.00%	10.39	0.3245	0.9322	1.5662	10.39	0.3245	0.9322	1.5662	10.39	0.3245	0.9322	1.5662
	0.25%	9.085	0.2866	0.9046	1.5878	4.187	0.2182	0.9533	0.8640	2.099	0.2046	0.9664	0.6827
	0.50%	3.932	0.1928	0.9336	0.9200	1.632	0.1149	0.9663	0.3844	1.218	0.0937	0.9526	0.3743
	0.75%	2.088	0.1334	0.9673	0.4195	0.830	0.0916	0.9733	0.2715	0.587	0.0324	0.9280	0.1616
45 °C	0.00%	96.09	0.2892	0.9579	1.0850	96.09	0.2892	0.9579	1.0850	96.09	0.2892	0.9579	1.0850
	0.25%	7.412	0.3239	0.9920	0.5217	5.25	0.2546	0.9914	0.4236	0.530	0.3003	0.9709	0.9307
	0.50%	0.2167	0.3521	0.9729	1.0518	0.705	0.1213	0.9924	0.1819	0.549	0.0986	0.9743	0.2865
	0.75%	−1.534	0.4381	0.9396	1.988	0.795	0.0719	0.9801	0.1826	0.3832	0.0531	0.9714	0.1631
65 °C	0.00%	20.49	0.3602	0.9497	1.4835	20.49	0.3602	0.9497	1.4835	20.49	0.3602	0.9497	1.4835
	0.25%	4.659	0.4032	0.9912	0.6814	3.458	0.2141	0.9905	0.3760	1.095	0.1287	0.9860	0.2744
	0.50%	1.877	0.3418	0.9914	0.6061	−0.120	0.1445	0.9809	0.3456	0.594	0.0267	0.9233	0.1380
	0.75%	−1.947	0.4873	0.9723	1.4734	−0.953	0.1616	0.9472	0.6807	0.598	0.0208	0.8451	0.1596

(1) For shear thinning (sh-thin) behavior:

$$\frac{d\tau}{d\gamma} = k * n * \gamma^{(n-1)} > 0 \cdots\cdots\cdots k * n > 0$$

$$\frac{d^2\tau}{d\gamma^2} = k * n(n-1) * \gamma^{(n-2)} < 0 \cdots\cdots\cdots k * n * (n-1) < 0$$

These conditions will be satisfied only if (0 < n < 1) and (k > 0) From the Eq. (2). When $\gamma^{\circ}=\infty \Longrightarrow \tau=\infty$. So, Herschel–Bulkley model doesn't satisfy the limitations condition on the maximum SS limit [18,19,36]. There for Herschel–Bulkley-model cannot be applied for sh-thin behavior [18,19] to determine YS as obtained in Table 4.

(2) For shear thickening (sh-thick) behavior:

$$\frac{d\tau}{d\gamma} = k * n * \gamma^{(n-1)} > 0 \cdots\cdots\cdots k * n > 0$$

$$\frac{d^2\tau}{d\gamma^2} = k * n(n-1) * \gamma^{(n-2)} > 0 \cdots\cdots\cdots k * n * (n-1) > 0$$

These conditions will be satisfied only if (1 < n < 2) and (k > 0) From the Eq. (2). When $\gamma^{\circ}=\infty \Longrightarrow \tau=\infty$. So, Herschel–Bulkley model satisfy all condition that present in Table 3 for sh-thick. Therefore Herschel–Bulkley model can be applied for sh-thick behavior.

From Table 5, it is shown that in case of sh-thin (n < 1), the (τ°< 0) which is impossible, But in case of the sh-thick (n > 1), the (τ°> 0) as it must to be. These values also indicated that the Herschel–Bulkley model cannot be used to estimate the rheological parameter of sh-thin behavior; it is used only for sh-thick behavior.

On the other hand, three main disadvantages exist in Herschel–Bulkley-model as the following: (i) Accuracy of Herschel–Bulkley-model is a very low at low and/or high SR [37] (ii) In case of the sh-thick; at a very low SR values the inclination of the curve approaches to "zero", leading to an overestimation of the values of YS values [35]; and (ii) analysis of the physical parameter "k" is a very difficult as it's dimension is ($Pa.S^n$), therefore it depends on the values of n, the "k" dimension is variable which have no physical meaning [35].

According to the disadvantage that illustrated above, empirical model with these properties must be introduced: (i) having positive values of YS; (ii) Avoid zero inclination; and (iii) having fixed dimension parameter [35]. Therefore, the use of another model like modified Bingham model can solve these problems [37,39,41].

3.2.2.3. Modified Bingham model. Data shown in Table 6 shows that for all C-Ps (π° >0), and this is accepted. Also, for C-Ps which have sh-thick behavior, the YS values in case of modified Bingham-model are lower than in case of Herschel–Bulkley-model, therefore the modified-Bingham-model solved the problem of the overestimation values of YS that computed by Herschel–Bulkley-model. The conditions that reported in Table 3 were also checked by this model.

Table 5
Rheological parameters of Herschel–Bulckley model for control and admixed cement pastes containing different doses from TG, SI and SII at different temperatures 25 °C, 45 °C and 65 °C.

Temperature (°C)	Dose (%)	Herschel–Bulckley model														
		TG					SI					SII				
		τ°	k	n	R^2	RMSE	τ°	k	n	R^2	RMSE	τ°	k	n	R^2	RMSE
25 °C	0.00%	2.064	4.322	0.435	0.982	0.834	2.064	4.322	0.435	0.982	0.834	2.064	4.322	0.435	0.982	0.834
	0.25%	−3.528	7.733	0.310	0.987	0.566	−1.09	2.717	0.448	0.997	0.193	−1.575	0.175	0.521	0.998	0.155
	0.50%	−2.392	3.552	0.375	0.994	0.285	−0.57	1.069	0.504	0.999	0.068	−1.356	1.378	0.416	0.999	0.047
	0.75%	−0.186	1.076	0.533	0.998	0.093	−0.57	0.651	0.559	0.998	0.076	−0.779	0.830	0.319	0.998	0.025
45 °C	0.00%	11.87	0.0171	1.693	0.993	0.443	11.87	0.0171	1.693	0.993	0.443	11.87	0.0171	1.693	0.993	0.443
	0.25%	8.353	0.154	1.178	0.994	0.436	5.755	0.157	1.115	0.992	0.405	2.696	0.025	1.599	0.994	0.418
	0.50%	2.571	0.038	1.538	0.996	0.401	1.016	0.063	1.154	0.994	0.161	0.9264	0.035	1.247	0.978	0.275
	0.75%	2.627	0.008	1.979	0.994	0.605	0.848	0.060	1.04	0.976	0.190	0.4612	0.037	1.083	0.971	0.169
65 °C	0.00%	23.37	0.0198	1.722	0.988	0.755	23.37	0.0198	1.722	0.988	0.755	23.37	0.0198	1.722	0.988	0.755
	0.25%	5.003	0.313	1.046	0.991	0.706	3.489	0.207	1.008	0.990	0.394	−0.059	0.511	0.683	0.997	0.113
	0.50%	2.527	0.216	1.11	0.992	0.559	0.360	0.060	1.209	0.986	0.321	−0.728	0.846	0.284	0.993	0.043
	0.75%	1.297	0.054	1.533	0.995	0.591	0.497	0.045	1.88	0.994	0.230	−4.914	4.906	0.070	0.991	0.040

Table 6
Rheological parameters of modified Bingham model for control and admixed cement pastes containing different doses from TG, SI and SII at different temperatures 25 °C, 45 °C and 65 °C.

Temperature (°C)	Dose (%)	Modified Bingham model														
		TG					SI					SII				
		τ°	μ	a	R^2	RMSE	τ°	μ	a	R^2	RMSE	τ°	μ	a	R^2	RMSE
25 °C	0.00%	7.177	0.066	−0.001	0.997	0.034	7.177	0.066	−0.001	0.997	0.034	7.177	0.066	−0.001	0.997	0.034
	0.25%	5.864	0.623	−0.006	0.994	0.413	2.413	0.403	−0.003	0.997	0.177	0.722	0.348	−0.003	0.997	0.193
	0.50%	2.028	0.391	−0.004	0.998	0.146	0.903	0.191	−0.002	0.993	0.171	0.525	0.166	−0.002	0.989	0.183
	0.75%	1.311	0.214	−0.001	0.993	0.204	0.343	0.142	−0.001	0.992	0.146	0.269	0.065	−0.001	0.991	0.057
45 °C	0.00%	11.68	0.072	0.004	0.992	0.468	11.68	0.072	0.004	0.992	0.468	11.68	0.072	0.004	0.992	0.468
	0.25%	8.087	0.253	0.0012	0.9950	0.4304	5.473	0.231	0.0004	0.992	0.430	2.342	0.110	0.0033	0.996	0.359
	0.50%	2.216	0.142	0.0036	0.9952	0.4623	0.961	0.094	0.0004	0.996	0.141	0.869	0.065	0.0005	0.981	0.254
	0.75%	2.455	0.021	0.0072	0.9940	0.5989	0.901	0.060	0.0001	0.981	0.184	0.482	0.042	0.0001	0.973	0.163
65 °C	0.00%	23.18	0.078	0.005	0.987	0.778	23.18	0.078	0.005	0.987	0.778	23.18	0.078	0.005	0.987	0.778
	0.25%	4.941	0.373	0.0005	0.989	0.700	3.573	0.202	0.0002	0.990	0.390	0.627	0.177	−0.001	0.995	0.167
	0.50%	2.377	0.289	0.0009	0.992	0.544	0.251	0.105	0.0006	0.987	0.310	0.373	0.049	−0.001	0.968	0.093
	0.75%	0.817	0.198	0.0050	0.994	0.690	0.404	0.019	0.0024	0.994	0.224	0.295	0.052	−0.001	0.972	0.070

$$\frac{d\tau}{d\gamma} = \mu + 2a\dot{\gamma}$$

$$\frac{d^2\tau}{d\gamma^2} = 2a$$

(1) For shear thinning (sh-thin) behavior:

$$\frac{d\tau}{d\gamma} = \mu + 2a\dot{\gamma} > 0$$

$$\frac{d^2\tau}{d\gamma^2} = 2a < 0 \cdots\cdots\cdots a < 0$$

(2) For shear thickening (sh-thick) behavior:

$$\frac{d\tau}{d\gamma} = \mu + 2a\dot{\gamma} > 0$$

$$\frac{d^2\tau}{d\gamma^2} = 2a > 0 \cdots\cdots\cdots a > 0$$

Such conditions will be satisfied only if (a < 0) in case of sh-thin and (a > 0) in case of sh-thick. It can be specified from the data outlined in Table 6, that the mix has a sh-thin/thick behavior according to the value of "a". Which is also proved by the value of "n" that derived from the Herschel–Bulkley-model as in case of (n < 1), it was found that (a < 0) which refers to sh-thin behavior. And also, in case of (n > 1), it was found that (a > 0) which refers to sh-thick behavior.

3.2.2.4. Vipulanandan (Hyperbolic) model. Hence the YS had negative values and the upper limit condition cannot be satisfied by using Herschel-Bulkley-model [18]. Hyperbolic-model Eq. (4) was established to fulfill the sh-thin condition [18]. As the model must satisfy the condition that illustrated in Table 3

$$\frac{d\tau}{d\dot{\gamma}} = \frac{(B + A\dot{\gamma}) - \dot{\gamma} * A}{(B + A\dot{\gamma})^2} = \frac{B}{(B + A\dot{\gamma})^2}$$

$$\frac{d^2\tau}{d\dot{\gamma}^2} = \frac{-2BA}{(B + A\dot{\gamma})^4}$$

(1) For shear thinning (sh-thin) behavior:

$$\frac{d\tau}{d\dot{\gamma}} = \frac{(B + A\dot{\gamma}) - \dot{\gamma} * A}{(B + A\dot{\gamma})^2} = \frac{B}{(B + A\dot{\gamma})^2} > 0 \cdots\cdots\cdots B > 0$$

$$\frac{d^2\tau}{d\dot{\gamma}^2} = \frac{-2BA}{(B + A\dot{\gamma})^4} < 0 \cdots\cdots\cdots A > 0$$

$$\text{Alsowhen}\dot{\gamma} = \infty \cdots\cdots\cdots \tau = \tau^{\circ} + \frac{1}{A}$$

(2) For shear thickening (sh-thick) behavior:

$$\frac{d\tau}{d\dot{\gamma}} = \frac{(B + A\dot{\gamma}) - \dot{\gamma} * A}{(B + A\dot{\gamma})^2} = \frac{B}{(B + A\dot{\gamma})^2} > 0 \cdots\cdots\cdots B > 0$$

$$\frac{d^2\tau}{d\dot{\gamma}^2} = \frac{-2BA}{(B + A\dot{\gamma})^4} > 0 \cdots\cdots\cdots A < 0$$

Hence Hyperbolic-model has a value to (τ) when ($\dot{\gamma}$= ∞), this model meets all conditions of sh-thin behavior described in Table 3, if (B > 0) and (A > 0). Hyperbolic-model cannot satisfy last condition for the sh-thick behavior since (τ) does not have infinite value when ($\dot{\gamma}$= ∞), but it can satisfy the first and second condition when (B > 0) and (A < 0).

Also, data presented in Table 7 for the Hyperbolic-Model indicate the behavior of the C-Ps (sh-thin/thick) according to the value of "A". From the values of Table 5 and Table 7, it was observed that (A > 0) when (n < 1) indicates the sh-thin behavior and (A < 0) when (n > 1) indicates the sh-thick behavior.

3.2.2.5. Comparison of models predictions. It can be examined from the R^2 and RMSE values for the various models that the Hyperbolic model has the best fitting curves as it has the maximum R^2 values.

3.2.3. Effects of different types of admixtures on yield stress values at different temperatures:

The Hyperbolic-model is used for calculating the YS values for all C-Ps according to the value of R^2. It was found that the YS value increased with increased temperature in the case of a control sample. This is due to an increase in SF's pozzolanic activity and hydration rate. Therefore, water demand and formation of further

Table 7
Rheological parameters of Hyperbolic model for control and admixed cement pastes containing different doses from TG, SI and SII at different temperatures 25 °C, 45 °C and 65 °C.

Temperature (°C)	Dose (%)	Hyperbolic model														
		TG					SI					SII				
		τ°	B	A	R^2	RMSE	τ°	B	A	R^2	RMSE	τ°	B	A	R^2	RMSE
25 °C	0.00%	6.605	1.155	0.029	0.989	0.633	6.605	1.155	0.029	0.989	0.633	6.605	1.155	0.029	0.989	0.633
	0.25%	4.448	0.976	0.0362	0.996	0.316	1.827	1.809	0.0427	0.999	0.078	0.294	2.223	0.0419	0.999	0.090
	0.50%	1.367	1.729	0.0516	0.998	0.148	0.622	3.976	0.0747	0.997	0.115	0.167	4.073	0.1014	0.996	0.112
	0.75%	1.007	3.61	0.062	0.996	0.142	0.160	5.592	0.0857	0.995	0.112	0.099	9.125	0.3184	0.999	0.018
45 °C	0.00%	11.1	6.398	−0.054	0.989	0.571	11.1	6.398	−0.054	0.989	0.571	11.1	6.398	−0.054	0.989	0.571
	0.25%	8.056	3.835	−0.0133	0.995	0.427	5.444	4.258	−0.006	0.991	0.431	2.041	6.02	−0.049	0.996	0.326
	0.50%	1.699	4.628	−0.3264	0.992	0.577	0.972	10.49	−0.004	0.998	0.133	0.896	15.07	−0.089	0.983	0.242
	0.75%	1.312	5.085	−0.0521	0.993	0.701	0.924	16.98	−0.054	0.982	0.181	0.512	24.61	−0.103	0.974	0.160
65 °C	0.00%	22.53	5.479	−0.049	0.985	0.839	22.53	5.479	−0.049	0.985	0.839	22.53	5.479	−0.049	0.985	0.839
	0.25%	4.933	2.666	−0.0032	0.991	0.700	3.589	4.983	−0.005	0.990	0.389	0.519	5.06	0.0451	0.996	0.152
	0.50%	2.389	3.44	−0.0091	0.991	0.620	0.264	9.297	−0.043	0.987	0.303	0.176	10.52	0.3937	0.985	0.062
	0.75%	0.108	3.343	−0.0235	0.991	0.840	0.026	12.95	−0.125	0.992	0.268	0.030	7.297	0.5164	0.995	0.027

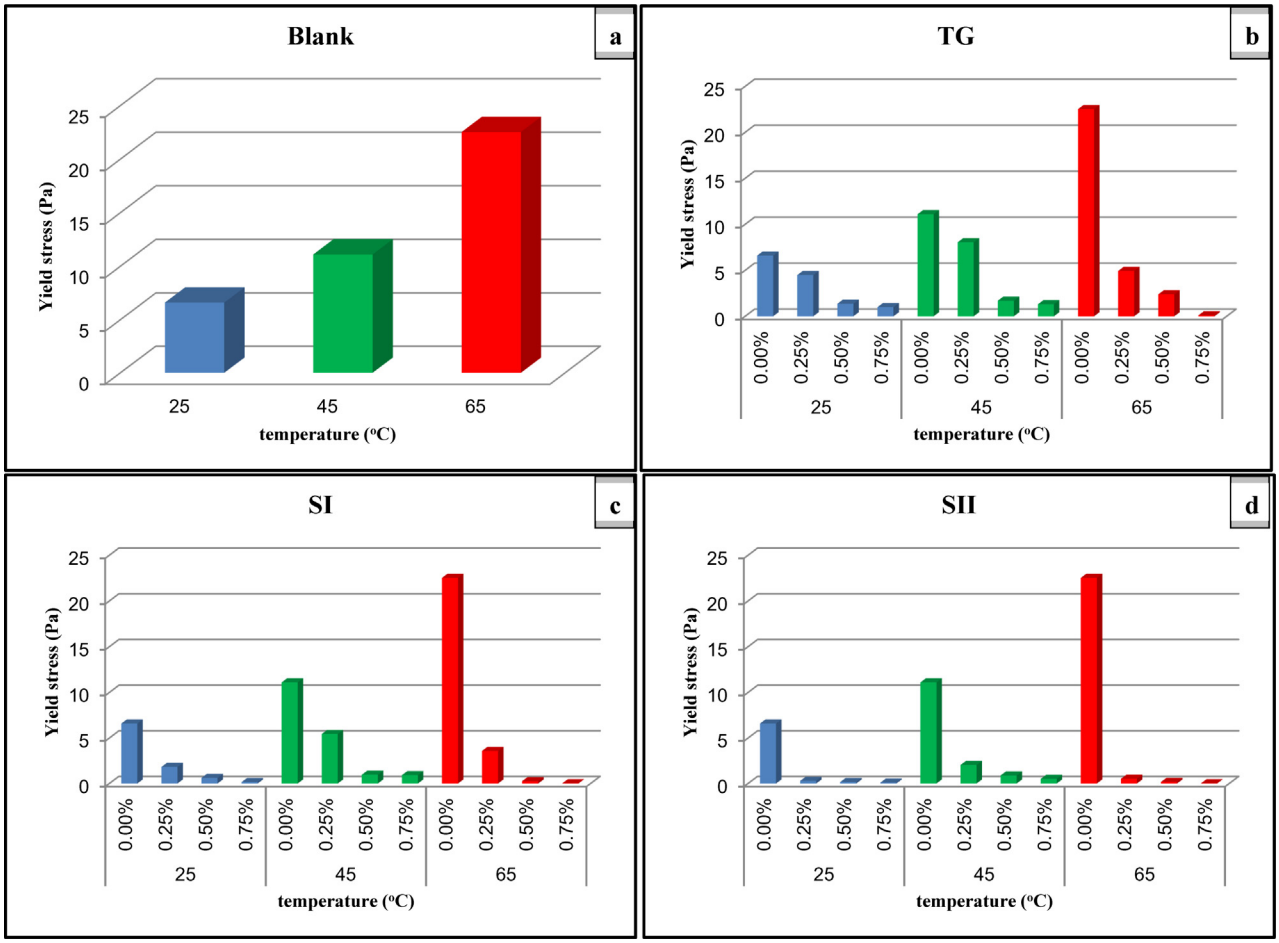

Fig. 8. Yield stress values for control and admixed cement paste containing different doses from TG, SI and SII at different temperatures.

hydration products were increased, leading to increment in the YS values as shown in Fig. 8a [6,27,42].

(8b-8d) showed YS values for admixed C-Ps at various temperatures (25 °C, 45 °C and 65 °C It can be observed that with increasing doses of a particular admixture, YS values decreased regardless of the temperature applied. That is because of the dispersion effect as shown above [23].

And it was also found that as the temperature rose to 45 °C, the YS increased. As the temperature rises, the rate of hydration products formation increases. This is the result of dissolving a variety of ions from the mineral phases of the cement molecules into aqueous solution as they come into contact with water, combining these ions to create hydration products. Raising the temperature will increase the ions diffusion rate and formations of hydration products rate which cause the YS values to increase [16]. The same result was reported before, that the formations of flocculated structures were vital factor for the initial flowability of C-Ps. At high temperature more flocculated phases were formed since of quicker dissolution of minerals as well as formation hydration products, also consumption of free water as it entrapped by flocculated structure. Thus, increasing the temperature decreases the initial flowability [16,43].

At 65 °C, YS values for all doses were found to be higher than that at 25 °C, resulting from early hydration as shown above. But the YS values at 65 °C are lower than 45 °C; this decrease is likely due to decrease the viscosity of free water at a higher temperature [42], and also higher temperature enhanced the thermal motion and reduced the interaction between cement grains [16,30,44].

It is understood that the introduction of the admixtures was intended to increase the initial flowability by adsorption on cement grain. At higher temperature, more ions are generated, which induce formation of many flocculated structures, then more admixtures are consumed and being inserted or incorporated into hydration products.

As shown in Fig. 8b-d, the YS values for admixed C-Ps are gradually decreased even at higher temperatures, since the retardation effect of higher doses of admixtures eliminates the acceleration effect of high temperatures [23]. Such admixtures can therefore be used to reduce the temperature effect. Also, it is also obvious that the YS values for various admixture forms are SII < SI < TG. This indicated that the new prepared superplacticizers at higher temperatures are very effective in enhancing the rheological properties of SF-BCPs.

3.2.4. The influence of different types of admixtures on the shear thinning / thickening actions of cement pastes at different temperatures:

In many operations sh-thick action becomes very important at a high SR, as it has many drawbacks [6,36,37]. When the viscosity increases with increasing SR, a significant amount of energy is required to accelerate the material's pumping. It can also break in the mixer, pump or pipes if the sh-thick happens during the pumping cycle. Therefore, controlling sh-thick behavior is necessary, in order to avoid broken of any system and any dangerous can occur on worksites [12].

In this part Herschel–Bulkley-model was used to identify sh-thin/thick behavior of cement pastes as a function of temperature and types & doses of chemical admixtures. It was found that the rheological properties (sh-thin/thick) are depends on the applied SR [37]. The possible theory for the sh-thick behavior, built on formation of hydro-clusters (order and disorder theory), which are temporary flocculation of small particles. At certain SR (critical shear rate), these clusters started to form. They cause increasing in the viscosity with increasing SR.

During a long time, sh-thin is described by several authors, as the shear made ordering of the suspended particles. When the Brownian forces (is the random motion of suspended particles in a solution, that resulting from collision of these particles with another fast-moving molecules in the solution) acting on the suspended particles are dominated by the hydrodynamic forces, the particles cannot become into a random packing [12,45]. As results several layers of particles will formed with only interstitial fluid in between these layers, this fluid between the layers cause decreasing in viscosity [12].

At high SR, the layers start to disappear and disordering is induced by the shear, causing of sh-thick [12,46–49]. High SR induce high hydrodynamic (lubrication), which overcoming repulsion forces between the particles and forming temporary assemblies of suspended particles, named as hydro-clusters [12,50,51]. At the same instance, particles can join with each other and leave the formed cluster. If a cluster is formed, jamming can occur, which leads to increase in the viscosity and stopping the flow of this suspended solution [12,52–54]. Therefore, it is concluded that sh-thick starts at the critical SR (at which the ratio between the hydrodynamic forces and the repulsive forces (which can be in many forms as Brownian, electrostatic or steric) becomes larger than one) [12,50,51].

At 25 °C, it was observed that the control paste has a sh-thin behavior but at high temperature (45 °C and 65 °C) has a sh-thick behavior. The sh-thin behavior is due to the finer particles of SF that can be introduced in the space between cement grains as the SF has average diameter 200 times lower than cement particle, therefore SF will reduce the friction between the cement particles by bearing effect [33]. Similar results are observed before, as using a proper amount of silica fume can reduce the viscosity and YS [6,33,55–57]. On the other hand, the sh-thick at a higher temperature is detected, as the pozzolanic activity of SF increases with increasing temperature as well as more hydration products is formed with consumption a high amount of free water, therefore increasing in viscosity is observed with increasing SR [6].

Recently, it has been found that using some types of chemical admixtures caused in sh-thick behavior of cement pastes. As the dispersing mechanisms (steric hindrance or electrostatic repulsion force) of admixtures are responsible for the sh-thin/thick behavior [6,58]. Mixtures acting by steric effect showed a greater sh-thick response than to those acting by electrostatic effect [33]. When the polymer adsorbs on cement grains, repulsive force occurs between them due to elastic and mixing components mechanisms [6,59,60]. When the space between two grains is equal to or higher than double the thickness of the polymer layer adsorption, cement grains can be considered as a dispersed medium. When cement grains try to approach each other, the "elastic component" of the steric hindrance part in admixture exhibits repulsive interactions between them. From another side, the "mixing component" of steric hindrance part resists this repulsion force [6]. Therefore, as the dose of admixture increase, the resistance of mixing part that occurs by un-adsorbed admixture polymers increases, cause formation flocculated structures as well as increasing the viscosity. This is perhaps the reason why the exponent "n" increased with the increase admixture dose.

The exponent "n" values with different doses of TG at different temperature were presented in Fig. 9a. It can be observed that the exponent "n" increased with increasing the TG doses as illustrated above, regardless of the temperature. At 25 °C, the pastes admixed with TG has a sh-thin behavior, that results from the dispersion action and retardation effect of TG. Then, the exponent "n" continued to increase with increasing temperature (45 °C and 65 °C) and the slurry changed from sh-thin to sh-thick behavior, due to the breakdown of TG layer by increasing the temperature and shearing rate then formation of hydration products. At 65 °C the sh-thick behavior is lower than at 45 °C, as at a high temperature the interaction between cement grains (hydro-cluster structures) is decrease, leading to decrease the sh-thick behavior.

It can be detected that as the dose of SI increase the "n" values increase, regardless of the temperature. Similar to TG, the pastes admixed with SI at 25 °C showed a sh-thin behavior. Also, as the temperature increases (45 °C and 65 °C), the ability for sh-thick behavior was increased as in Fig. 9b. At low doses (0.25%), the sh-thick behavior of at 65 °C is lower than at 45 °C. But by increasing the dose (0.50% and 0.75%), the ability of the sh-thick behavior was increased at 65 °C than 45 °C. This is due to increasing

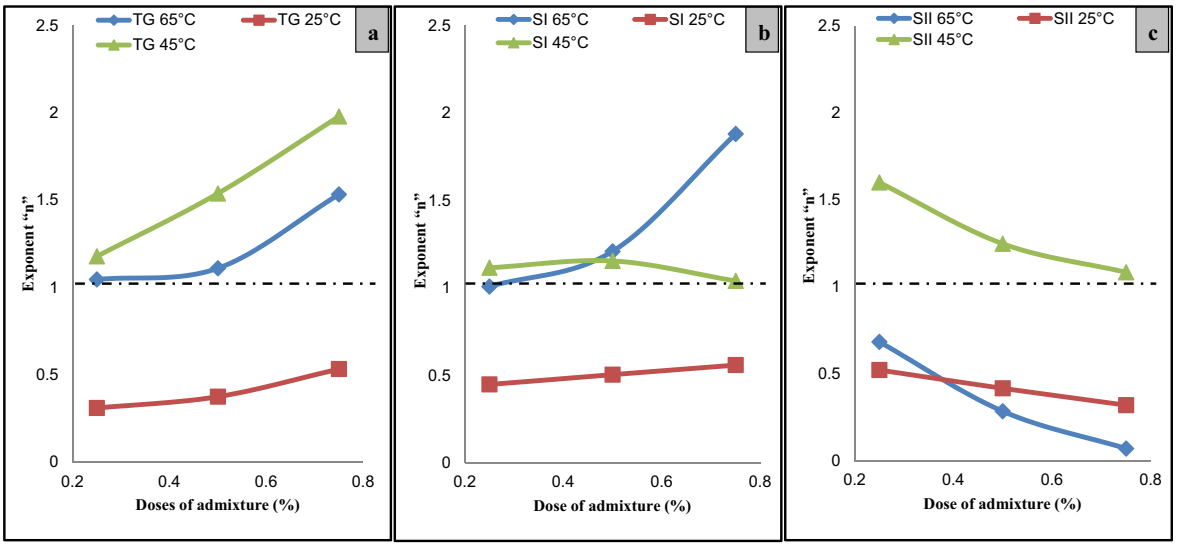

Fig. 9. Exponent "n" values for admixed cement paste containing different doses from TG, SI and SII at different temperatures.

temperature with SR leads to breakdown the polymer layer, also the high steric hindrance effect of SI as it is a high phenol content, all of this increase the amount of un-absorbed polymer in aqueous solution and increase the resistance of mixing component of steric hindrance part cause sh-thick behavior.

On the other hand Fig. 9c shown that as the dose of SII increase, the exponent "n" values decreased regardless the curing temperature. This is due to the weak effect of steric hindrance (in SII), as SII is low phenol content. Also, as the dose of SII increase, the retardation effect increase. At 25 °C and 65 °C the cement pastes admixed with SII show a sh-thin effect. The sh-thin behavior is due to retardation effect at 25 °C, also at 65 °C is due to increasing the thermal motion and decreasing the interaction forces. At lower doses (0.25%), the sh-thin behavior at 65 °C is lower than at 25 °C, but by increasing the doses (0.50% and 0.75%) with increasing temperature (from 25 °C to 65 °C) make the sh-thin behavior of at 65 °C is higher than at 25 °C. As at a low dose there are enough amounts of SII to make retardation effect, but at a higher dose there are two factors are affected (i) retardation effect of higher dose; and (ii) the thermal motion effect at a high temperature.

4. Conclusion:

(1) The spread area of control sample is lower than admixed C-Ps. The workability of SII is higher than SI and TG. The critical dose is 0.75% for SI and 0.50% for SII, but cement slurries admixed with TG do not reach to critical dose till 1.00%, this give indication about a high efficiency of small doses of prepared chemical admixtures.

(2) For control and admixed C-Ps, increasing the SR is accompanied by increasing in the SS. As the dose of admixture increases the flow curve shifts to lower values of SS. Therefore, the energy required to accelerate the flowing of admixed C-Ps is lower than control sample. At the same dose the SS values is arranged as the following SII < SI < TG, this give indication about powerful action of prepared admixtures.

(3) As the temperature increases, the workability of control and admixed C-Ps decreases, due to increase the rate of hydration and pozzolanic activity with increasing temperatures. High SR with high temperature, make the SS of the C-Ps admixed with TG increases with increasing the dose, as the high temperature with shear rate accelerate the breakdown of polymer layers make the concentration of polymer in interstitial solution increases as well as viscosity. This problem does not present in SI and SII, which reflects to the high stability of the prepared admixture against high shear rate and high temperature.

(4) According to R^2 values, rheological data fit the hyperbolic-model more than other models; therefore, the obtained YS values of hyperbolic-model seem to be more accurate.

References

[1] Abo-El-Enein SA, El-Hosiny FI, El-Gamal SMA, Amin MS, Ramadan M. Gamma radiation shielding, fire resistance and physicochemical characteristics of Portland cement pastes modified with synthesized Fe2O3 and ZnO nanoparticles. Constr Build Mater 2018;173:687–706.

[2] Ramadan M, Amin MS, Sayed MA. Superior physico-mechanical, fire resistivity, morphological characteristics and gamma radiation shielding of hardened OPC pastes incorporating ZnFe2O4 spinel nanoparticles 2020/02/20/. Constr Build Mater 2020;234:117807.

[3] Ma J, Dietz J, Dehn F. Ultra high performance self compacting concrete. Lacer 2002;7:33–42.

[4] Abo-El-Enein S, Hanafi S, El-Hosiny F, El-Mosallamy E-S-H, Amin M. Effect of some acrylate—poly (ethylene glycol) copolymers as superplasticizers on the mechanical and surface properties of Portland cement pastes. Adsorpt Sci Technol 2005;23(3):245–54.

[5] Uysal M, Sumer M. Performance of self-compacting concrete containing different mineral admixtures. Constr Build Mater 2011;25(11):4112–20.

[6] Shahriar A, Nehdi M. Effect of supplementary cementitious materials on rheology of oil well cement slurries. Adv Civ Eng Mater 2014;3(1):454–78.

[7] Hazem M, Hashem F, El-Gamal S, Amin M. Mechanical and microstructure characteristics development of hardened oil well cement pastes incorporating fly ash and silica fume at elevated temperatures. J Taibah Univ Sci 2020;14 (1):155–67.

[8] Mohsen A, Aiad I, El-Hossiny F, Habib A. Evaluating the mechanical properties of admixed blended cement pastes and estimating its kinetics of hydration by different techniques. Egypt J Pet 2020.

[9] Habib A, Aiad I, El-Hosiny F, El-Aziz AA. Development of the fire resistance and mechanical characteristics of silica fume-blended cement pastes using some chemical admixtures. Constr Build Mater 2018;181:163–74.

[10] Aiad I, Hafiz A. Structural effect of prepared and commercial superplasticizers on performance of cement pastes. J Appl Polym Sci 2003;90(2):482–7.

[11] Heikal M, Morsy MS, Aiad I. Effect of treatment temperature on the early hydration characteristics of superplasticized silica fume blended cement pastes 2005/04/01/. Cem Concr Res 2005.;35(4):680–7.

[12] Feys D, Verhoeven R, De Schutter G. Why is fresh self-compacting concrete shear thickening?. Cem Concr Res 2009;39(6):510–23.

[13] Tattersall GH, Banfill PF. The rheology of fresh concrete (no. Monograph); 1983.

[14] Tattersall G. The rationale of a two-point workability test. Mag Concr Res 1973;25(84):169–72.

[15] Yahia A, Khayat K. Analytical models for estimating yield stress of high-performance pseudoplastic grout. Cem Concr Res 2001;31(5):731–8.

[16] Zhang Y, Kong X, Gao L, Wang J. Rheological behaviors of fresh cement pastes with polycarboxylate superplasticizer. J Wuhan Univ Technol-Mater Sci Ed 2016;31(2):286–99.

[17] Nehdi M, Rahman M-A. Estimating rheological properties of cement pastes using various rheological models for different test geometry, gap and surface friction. Cem Concr Res 2004;34(11):1993–2007.

[18] Mohammed AS. Vipulanandan model for the rheological properties with ultimate shear stress of oil well cement modified with nanoclay 2018/09/01/. Egypt J Pet 2018;27(3):335–47.

[19] Mohammed AS. Effect of temperature on the rheological properties with shear stress limit of iron oxide nanoparticle modified bentonite drilling muds 2017/09/01/. Egypt J Pet 2017;26(3):791–802.

[20] Awad AH, Abdellatif MH. Assessment of mechanical and physical properties of LDPE reinforced with marble dust 2019/09/15/. Compos B Eng 2019;173:106948.

[21] Habib A, Aiad I, Youssef T, Abd El-Aziz A. Effect of some chemical admixtures on the physico-chemical and rheological properties of oil well cement pastes. Constr Build Mater 2016;120:80–8.

[22] Mohsen A, Abdel-Gawwad HA, Ramadan M. Performance, radiation shielding, and anti-fungal activity of alkali-activated slag individually modified with zinc oxide and zinc ferrite nano-particles. Constr Build Mater 2020;257:119584.

[23] Flatt R. Towards a prediction of superplasticized concrete rheology. Mater Struct 2004;37(5):289–300.

[24] Houst YF et al. Design and function of novel superplasticizers for more durable high performance concrete (superplast project). Cem Concr Res 2008;38 (10):1197–209.

[25] Han S, Yan P, Kong X. Study on the compatibility of cement-superplasticizer system based on the amount of free solution. Sci China Technol Sci 2011;54 (1):183–9.

[26] Yoshioka K, Sakai E, Daimon M, Kitahara A. Role of steric hindrance in the performance of superplasticizers for concrete. J Am Ceram Soc 1997;80 (10):2667–71.

[27] Heikal M, Morsy M, Aiad I. Effect of treatment temperature on the early hydration characteristics of superplasticized silica fume blended cement pastes. Cem Concr Res 2005;35(4):680–7.

[28] Daimon M, Roy DM. Rheological properties of cement mixes: II. Zeta potential and preliminary viscosity studies. Cem Concr Res 1979;9(1):103–9.

[29] Lei L, Plank J. Synthesis, working mechanism and effectiveness of a novel cycloaliphatic superplasticizer for concrete. Cem Concr Res 2012;42 (1):118–23.

[30] Gołaszewski J, Szwabowski J. Influence of superplasticizers on rheological behaviour of fresh cement mortars. Cem Concr Res 2004;34(2):235–48.

[31] Nawa T, Ichiboji H, Kinoshita M. Influence of temperature on fluidity of cement paste containing superplasticizer with polyethylene oxide graft chains. Special Publ 2000;195:181–94.

[32] Kinoshita M, Nawa T. Effect of chemical structure on fluidizing mechanism of concrete superplasticizer containing polyethylene oxide graft chains. Special Publ 2000;195:163–80.

[33] Yahia A. Shear-thickening behavior of high-performance cement grouts—Influencing mix-design parameters. Cem Concr Res 2011;41(3):230–5.

[34] Aiad I, El-Sabbagh A, Adawy A, Shafek S, Abo-EL-Enein S. Effect of some prepared superplasticizers on the rheological properties of oil well cement slurries. Egypt J Pet 2018;27(4):1061–6.

[35] Feys D, Verhoeven R, De Schutter G. Evaluation of time independent rheological models applicable to fresh self-compacting concrete. Appl Rheol 2007; 17(5): 56244-1-56244-10.

[36] Vipulanandan C, Mohammed A. Rheological properties of piezoresistive smart cement slurry modified with iron-oxide nanoparticles for oil-well applications. J Test Eval 2017;45(6):2050–60.

[37] Bouras R, Kaci A, Chaouche M. Influence of viscosity modifying admixtures on the rheological behavior of cement and mortar pastes. Korea-Australia Rheol J 2012;24(1):35–44.
[38] Feys D, Verhoeven R, De Schutter G. Fresh self compacting concrete, a shear thickening material. Cem Concr Res 2008;38(7):920–9.
[39] Yahia A, Khayat K. Experiment design to evaluate interaction of high-range water-reducer and antiwashout admixture in high-performance cement grout. Cem Concr Res 2001;31(5):749–57.
[40] Vipulanandan C, Mohammed A. Hyperbolic rheological model with shear stress limit for acrylamide polymer modified bentonite drilling muds. J Petrol Sci Eng 2014;122:38–47.
[41] Atzeni C, Massidda L, Sanna U. Comparison between rheological models for portland cement pastes. Cem Concr Res 1985;15(3):511–9.
[42] Hodne H, Saasen A, Strand S. Rheological properties of high temperature oil well cement slurries. Ann Trans-Nordic Rheol Soc 2001;8:31–8.
[43] Kong X, Zhang Y, Hou S. Study on the rheological properties of Portland cement pastes with polycarboxylate superplasticizers. Rheol Acta 2013;52(7):707–18.
[44] Petit J-Y, Wirquin E, Duthoit B. Influence of temperature on yield value of highly flowable micromortars made with sulfonate-based superplasticizers. Cem Concr Res 2005;35(2):256–66.
[45] Rastogi SR, Wagner NJ, Lustig SR. Rheology, self-diffusion, and microstructure of charged colloids under simple shear by massively parallel nonequilibrium Brownian dynamics. J Chem Phys 1996;104(22):9234–48.
[46] Hoffman R. Discontinuous and dilatant viscosity behavior in concentrated suspensions. I. Observation of a flow instability. Trans Soc Rheol 1972;16 (1):155–73.
[47] Hoffman R. Discontinuous and dilatant viscosity behavior in concentrated suspensions. II. Theory and experimental tests. J Colloid Interface Sci 1974;46 (3):491–506.
[48] Laun H et al. Rheological and small angle neutron scattering investigation of shear-induced particle structures of concentrated polymer dispersions submitted to plane Poiseuille and Couette flow a. J Rheol 1992;36(4):743–87.
[49] Boersma WH, Laven J, Stein HN. Shear thickening (dilatancy) in concentrated dispersions. AIChE J 1990;36(3):321–32.
[50] Maranzano BJ, Wagner NJ. The effects of particle size on reversible shear thickening of concentrated colloidal dispersions. J Chem Phys 2001;114 (23):10514–27.
[51] Bossis G, Brady J. The rheology of Brownian suspensions. J Chem Phys 1989;91 (3):1866–74.
[52] Liu A, Nagel S. Nonlinear dynamics—jamming is not just cool any more. Nature 1998;396:21.
[53] Cates M, Wittmer J, Bouchaud J-P, Claudin P. Jamming, force chains, and fragile matter. Phys Rev Lett 1998;81(9):1841.
[54] Egres RG, Wagner NJ. The rheology and microstructure of acicular precipitated calcium carbonate colloidal suspensions through the shear thickening transition. J Rheol 2005;49(3):719–46.
[55] Daukšys M, Skripkiūnas G, Ivanauskas E. Microsilica and plasticizing admixtures influence on cement slurry dilatancy. Mater Sci (Medžiagotyra) 2008;14(2):143–50.
[56] Yahia A, Khayat K. Applicability of rheological models to high-performance grouts containing supplementary cementitious materials and viscosity enhancing admixture. Mater Struct 2003;36(6):402–12.
[57] Khayat K, Yahia A, Sayed M. Effect of supplementary cementitious materials on rheological properties, bleeding, and strength of structural grout. ACI Mater J 2008;105(6):585.
[58] Cyr M, Legrand C, Mouret M. Study of the shear thickening effect of superplasticizers on the rheological behaviour of cement pastes containing or not mineral additives. Cem Concr Res 2000;30(9):1477–83.
[59] Al-Martini S. Investigation on rheology of cement paste and concrete at high temperature (no. 08); 2009.
[60] Yamada K. The effects of naphthalene sulfonate type and polycarboxylate type superplasticizers on the fluidity of belite-rich cement concrete. In: Proceedings of the International Workshop on Self-Compacting Concrete; 1988, pp. 201-210.

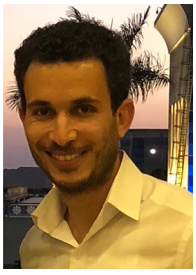

Alaa Mohsen